

## Introduction

### SPATIAL VARIABILITY EXISTS IN SOIL

- Maize yield and fertilizer requirement vary spatially (Machado et al., 2002), so precision agriculture techniques can be used to estimate and apply the economic optimum nitrogen (N) rate variably over space and time (Holland & Schepers, 2010).
- Knowledge of plant height is generally a strong indicator of how soil spatial variability affects crop growth and yield potential (Machado et al., 2002), especially when it is used in combination with spectral indices (Sharma et al., 2016).
- Leaf area index (LAI), defined as the green leaf area per unit horizontal soil area (Daughtry et al., 1992; Watson, 1947), and above-ground biomass are two common biophysical parameters of interest, largely because they play a key role in plant biophysical processes and influence the spectral reflectance of vegetation canopies (Baret et al., 2007).

- Accurate estimates of crop height, above-ground biomass, and/or LAI are critical for informing remote sensing algorithms and crop models (Baret et al., 2007; Casa et al., 2012; Fang et al., 2011), which can be used to predict crop N status across space.

### USING SENSORS FOR ESTIMATING BIOPHYSICAL PARAMETERS – MOTIVATION

- Measuring above-ground biomass and LAI via destructive methods is both time consuming and costly, especially as the growth stage progresses and there is more plant material to handle.
- There is strong interest in developing models for estimating these biophysical parameters using sensors, largely because it is the only practical method for characterizing them at scale.
- There are several nondestructive sensor-based methods published in recent literature to estimate plant height, LAI, and/or above-ground biomass (references available upon request), some of which include:
  - Optical spectral sensors
  - Spectral imagers – focus of this experiment (Figure 1)
    - Structured light/depth cameras (e.g., Microsoft Kinect®)
    - 3D reconstruction/Structure from Motion
    - Acoustic height sensors
    - Terrestrial laser scanners
- There are tradeoffs for each of these methods related to accuracy, scale, processing power, and/or implementation feasibility for estimating plant height, LAI, or above-ground biomass.
- Prediction models that use spectral data to predict plant biophysical parameters tend to over-fit and are generally constrained to local conditions, limiting their use under varying conditions (e.g., growth stages, variety/hybrid, soil color etc.).



Figure 1: Muhammad Tahir (right), Aicam Laacouri (middle), and myself (left) preparing the hexacopter and gimbal-mounted hyperspectral camera (inset photo) for aerial image acquisition.

## Objectives

- Investigate the relationships among maize height, LAI, above-ground biomass, and spectral reflectance during early growth stages (V5 - V10).
- Determine the reliability of spectral imagery to predict height, LAI, and biomass.

## Methods

### FIELD SITE AND TREATMENTS

- An experiment was conducted in 2017 at the Agricultural Ecology Research Farm at the Southern Research and Outreach Center near Waseca, MN.
- Four N fertilizer rates (0, 67, 135, and 202 kg N ha<sup>-1</sup>) were applied to a total of eight plots to ensure differences in plant growth among treatments.

### PLANT SAMPLING

- In each treatment plot, six maize plants were chosen for sampling. Painted stakes were placed between corn rows and aligned with the North-most and South-most plants to be sampled; every third plant in each row was sampled (Figure 2).
- Plant height and LAI (LI-COR LAI-2000; Lincoln, NE) were measured for each plant (n=48) at the V5, V8, and V10 growth stages.
- Following all other field measurements and image acquisition, plants were cut at ground-level and placed in a 100° C oven for drying.
- After drying for several days, samples were weighed to determine above-ground biomass (dry weight basis); note that above-ground biomass at V5 was consolidated by plot (n=6).

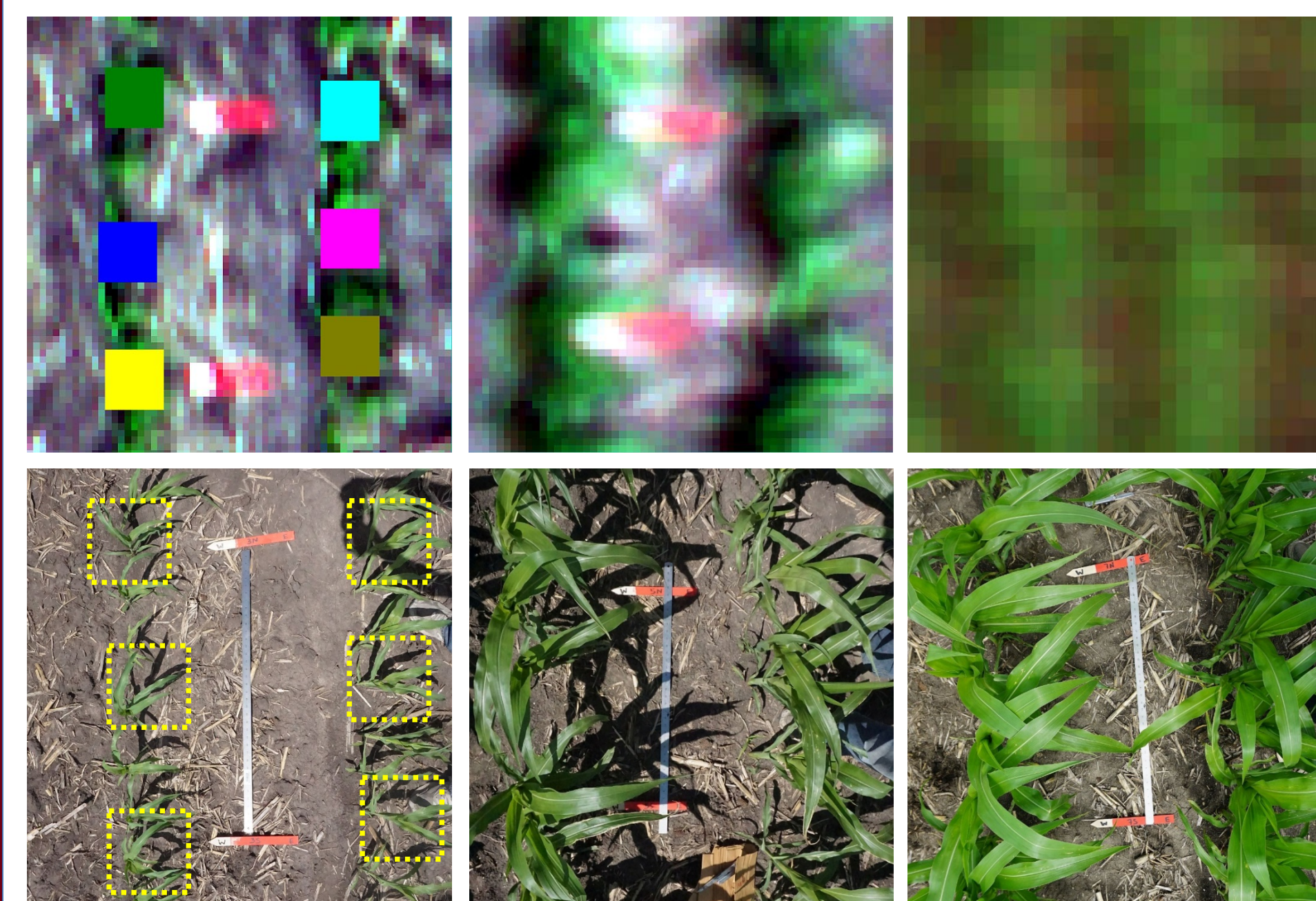


Figure 2: Hyperspectral aerial imagery (top row) and ground-photos (bottom row) of sampling areas at V5 (left), V8 (middle), and V10 (right) growth stages. Plot stakes were placed on the ground to identify the plants to be sampled in the aerial imagery. Boxes in the V5 column indicate the sampled plants.

### IMAGE ACQUISITION

- Hyperspectral aerial images (2.1 nm spectral resolution) were captured with a gimbal-stabilized Pika II line-scanning hyperspectral camera (Resonon, Inc.; Bozeman, MT) mounted on an unmanned hexacopter (DJI Matrice 600 Pro, Nanshan District, Shenzhen, China; Figure 1).
- DJI Ground Station Pro (iPad app) was used to create and execute flight plans for controlling altitude, heading, and ground speed (Table 1).
- Grey reference panels with known reflective properties were placed in the study area prior to image capture; panels were 60 x 60 cm and the surface was 50% BaSO<sub>4</sub>/50% grey paint by weight.

Table 1: Camera and flight specifications for each growth stage/sampling date.

Growth Stage	Date	Camera Framerate	Flight Altitude (m)	Ground Speed (m s <sup>-1</sup> )	Ground Sampling Distance
V5	15 June 2017	99	30	2.5	2.5 cm
V8	26 June 2017	91	30	2.5	2.7 cm
V10	01 July 2017	109	90	9.0	8.3 cm

### IMAGE PROCESSING

- Radiometric correction was performed via SpectronPro software (Resonon, Inc.; Bozeman, MT) using the calibration file provided by Resonon for the specific camera and lens that were used.
- Pixels representing the grey reference panels were used to convert spectral radiance to surface reflectance across all images.
- Imagery was visually inspected to determine the plants that were chosen for sampling; ENVI software version 5.2 (Harris Geospatial Solutions, Inc.) was used to create bounding squares around each sampled plant (see V5 column of Figure 2).
- Bounding squares for the image data were 9 x 9 pixels in size (~550 cm<sup>2</sup>) for the V5 and V8 growth stages, and 3 x 3 pixels in size (~620 cm<sup>2</sup>) for the V10 growth stage.
- Only spectral data extracted from the area of each sampled plant's bounding square were used for analysis.
- The Improved Modified Chlorophyll Absorption Ratio Index (MCARI2; Equation 1) was applied to each pixel; MCARI2 incorporates a soil adjustment factor while preserving sensitivity to LAI and resistance to chlorophyll influence and has been shown to be a good predictor of green LAI (Haboudane et al., 2004).

Equation 1: MCARI2 spectral vegetation index.

$$MCARI2 = \frac{1.5[2.5(\rho_{800} - \rho_{670}) - 1.3(\rho_{800} - \rho_{550})]}{\sqrt{(2 * \rho_{800} + 1)^2 - (6 * \rho_{800} - 5 * \sqrt{\rho_{670}}) - 0.5}}$$

## Results

### PLANT SAMPLE MEASUREMENTS

- Variability among plant samples within sampling date was substantially greater as growth stage progressed from V5 to V8 to V10, especially for above-ground biomass and LAI (Figure 3).
- Plant height and above-ground biomass were most closely related of all biophysical parameters ( $R^2 = 0.87$ ); as plant height increased, above-ground biomass increased exponentially.
- The kernel density estimates (i.e., probability) for plant height and MCARI2 are similar, but those for above-ground biomass and LAI are skewed and not similar at V8 and V10.

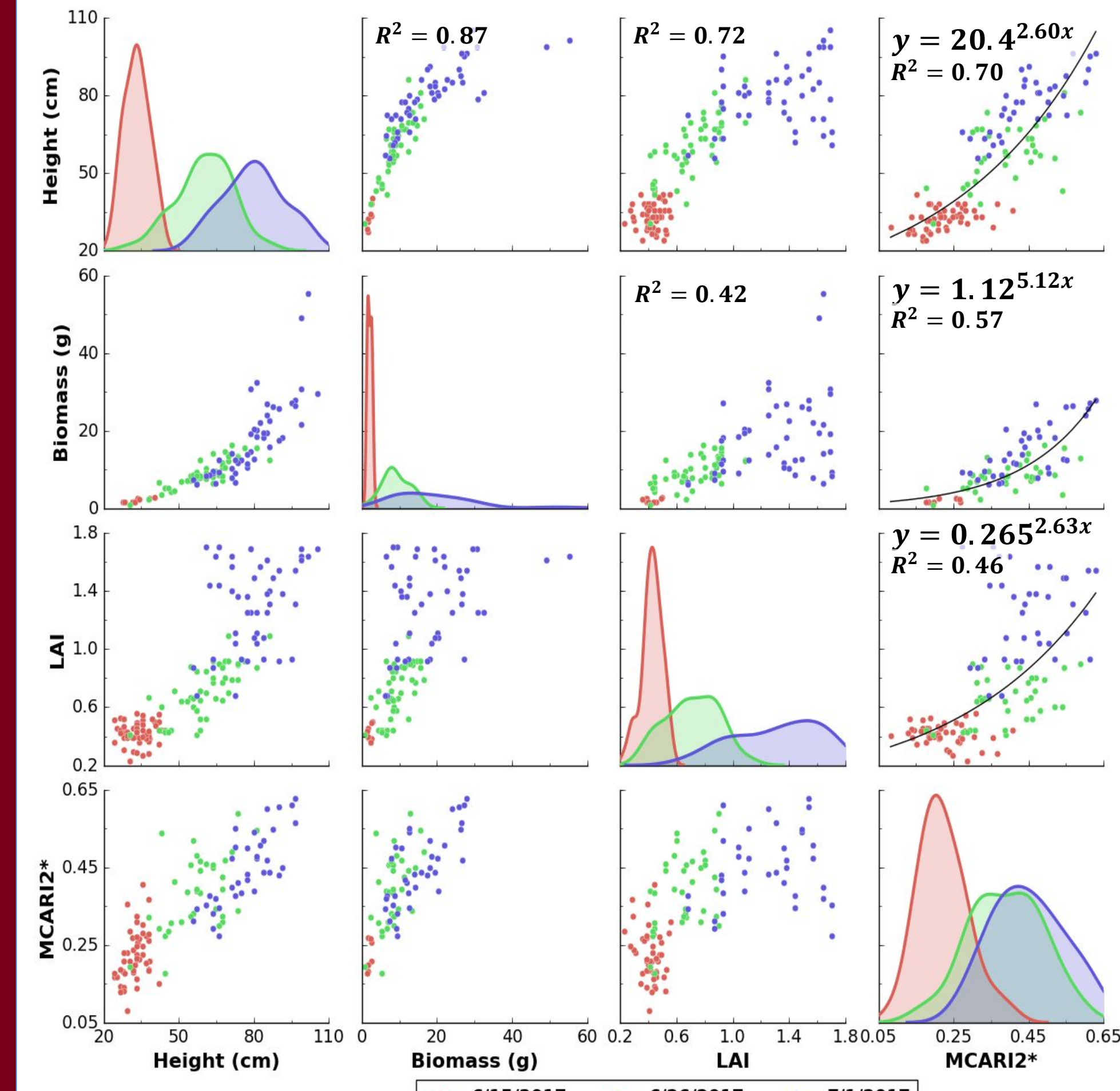


Figure 3: Scatterplot matrix illustrating relationships among plant height, above-ground biomass, leaf area index (LAI), and Improved Modified Chlorophyll Absorption Ratio Index (MCARI2). Plots on the diagonal are kernel density estimates illustrating relative probability of occurrence for respective variables. Colors represent samples collected at different growth stages (i.e., V5, V8, and V10). \*Note: MCARI2 is the only variable indirectly measured (via spectral data).

### PREDICTING BIOPHYSICAL PARAMETERS WITH SPECTRAL INFORMATION

- An exponential curve best explained the relationships between MCARI2 each of the three plant biophysical parameters (Figure 3).
- Of the three biophysical parameters measured, plant height had the closest relationship with MCARI2 ( $R^2 = 0.70$ ), followed by above-ground biomass ( $R^2 = 0.57$ ), then by LAI ( $R^2 = 0.46$ ).
- There was a tendency of all three biophysical parameters to be slightly overestimated with low measured/predicted values and underestimated with high measured/predicted values; evidence of this can be seen in Figure 4 with the less-steep slopes of the best-fit lines (black) compared to the 1:1 line (red).
- The 95% confidence intervals for the best-fit line between measured and predicted values were wider for the lowest and highest values compared to intermediate values (Figure 4).
- The root mean square error (RMSE) between measured and predicted values increased as growth stage progressed (Figure 5).
- Above-ground biomass at V5 had a higher RMSE than at either V8 or V10, but this was attributed to the small sample size (n=7) at that growth stage (Figure 5).

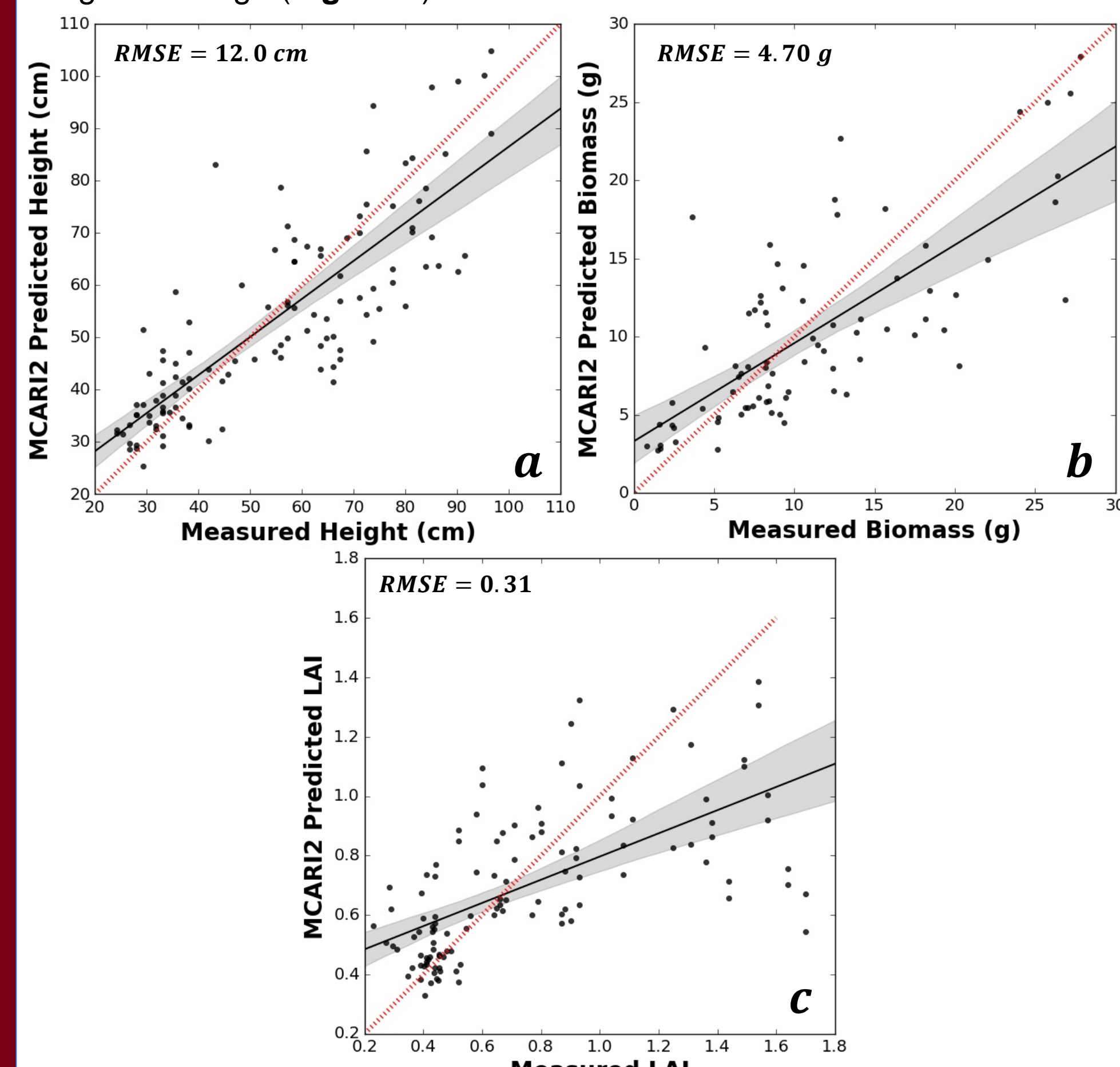


Figure 4: Measured versus MCARI2 predicted values for plant height (a), above-ground biomass (b), and leaf area index (c). The black line represents the best-fit between measured and predicted data points, the black shadow area represents a 95% confidence interval, and the red line represents a perfect 1:1 relationship.

## Results

### CROSS-VALIDATION

- A cross-validation approach was implemented that compared measured and predicted measurements after randomly assigning 90% of the values to a training dataset and the remaining 10% to a test dataset. Cross-validation was performed iteratively for each measurement until every sample was included in a test dataset (each iteration was independent of any other).
- The mean RMSE values from the cross-validation were less than the RMSE values from the full dataset (Figure 5), indicating that the reported prediction models do not over-fit the measured data.

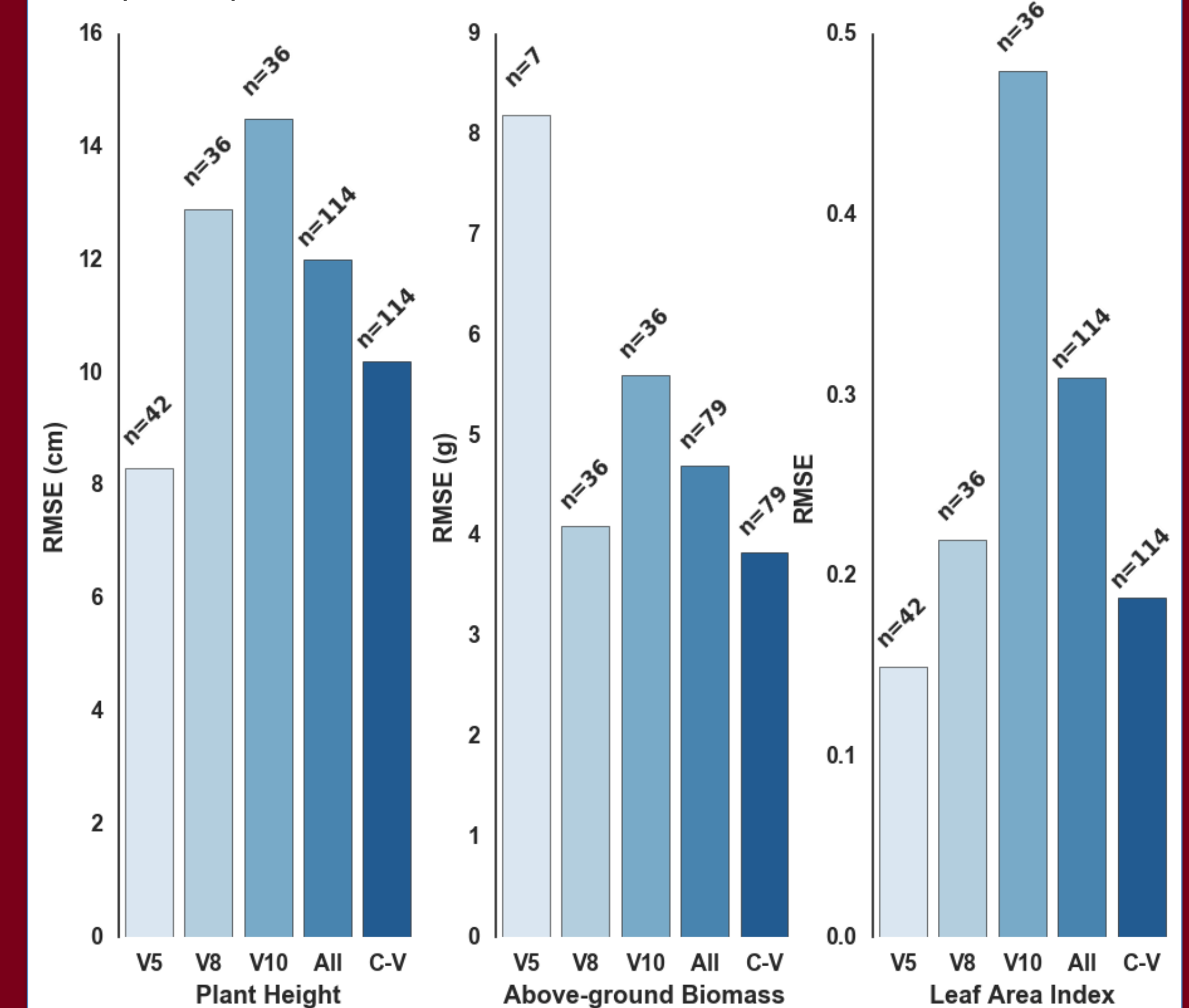


Figure 5: Root mean square error (RMSE) between MCARI2 and each biophysical measurement within growth stage. Cross-validation is denoted by "C-V", and the number of samples that were used is labeled above each bar.

## Conclusions

- The MCARI2 spectral index extracted from high resolution, narrowband aerial imagery produced satisfactory results for estimating plant height, above-ground biomass, and LAI.
- The measured/predicted plant height best-fit line had a closer relationship to the perfect 1:1 line than either above-ground biomass or LAI, which suggests that estimating plant height via MCARI2 is more accurate than estimating either above-ground biomass or LAI.
- It is unclear how well above-ground biomass can be predicted at the V5 growth stage from this experiment due to a small number of samples.
- Error between measured and predicted values increased as growth stage progressed, especially for biomass and LAI; this suggests that perhaps a separate model should be utilized after V8 (e.g., nearly all biomass samples > 15 g and nearly all LAI samples > 1.2 were underestimated).
- The prediction models reported herein did not over-fit the measured data (determined via cross-validation), but it is clear that predictions were generally overestimated at V5 and underestimated at V10.
- The approach described herein for predicting plant biophysical parameters is a viable option for reliably informing remote sensing algorithms and crop models, but variability of such estimations should be considered when interpreting the final precision N fertilizer recommendations.

### FUTURE DIRECTION

- The full hyperspectral dataset (240 bands from ~400 – ~900 nm) will be used to model these same biophysical parameters to determine if models can be improved.
- We plan to use these approaches in a future experiment to calibrate remote sensing algorithms and crop systems models for estimating optimum rates of N fertilizer during the crop season.

### ACKNOWLEDGEMENTS

Funding provided by MnDRIVE Global Food Ventures Fellowship and University of Minnesota Informatics Institute MnDRIVE PhD Graduate Assistantship. A special thanks to Ali Moghimi of Ce Yang's Agricultural Robotics lab for assistance and insight on many aspects of this project.

### WORKS CITED

- Baret, F., Houles, V., & Guérif, M. (2007). Quantification of plant stress using remote sensing observations and crop models: The case of nitrogen management. *Journal of Experimental Botany*, 58(4), 869–880. <https://doi.org/10.1093/jxb/erj231>
- Daughtry, C. S. T., Gallo, K. P., Goward, S. N., Prince, S. D., & Kustas, W. P. (1992). Spectral estimates of absorbed radiation and phytomass production in corn and soybean canopies. *Remote Sensing of Environment*, 39(2), 141–152. [https://doi.org/10.1016/0034-4257\(92\)90132-4](https://doi.org/10.1016/0034-4257(92)90132-4)
- Haboudane, D., Miller, J. R., Pattey, E., Zarco-Tejada, P. J., & Strachan, I. B. (2004). Hyperspectral vegetation indices and novel algorithms for predicting green LAI of crop canopies: modeling and validation in the context of precision agriculture. *Remote Sensing of Environment*, 90(3), 337–352. <https://doi.org/10.1016/j.rse.2003.12.013>
- Holland, K. H., & Schepers, J. S. (2010). Derivation of a variable rate nitrogen application model for in-season fertilization of corn. *Agronomy Journal*, 102(5), 1415–1424. <https://doi.org/10.2134/agronj2010.0015>
- Machado, S., Bynum, E. D., Archer, T. L., Lascano, R. J., Wilson, L. T., Bordovsky, J., Xu, W. (2002). Spatial and temporal variability of corn growth and grain yield: implications for site-specific farming. *Crop Science*, 42(5), 1564–1576. <https://doi.org/10.2135/cropsci2002.1564>
- Sharma, L. K., Bu, H., Franzen, D. W., & Denton, A. (2016). Use of corn height measured with an acoustic sensor improves yield estimation with ground based active optical sensors. *Computers and Electronics in Agriculture*, 124, 254–262. <https://doi.org/10.1016/j.compag.2016.04.016>
- Watson, D. J. (1947). Comparative Physiological Studies on the Growth of Field Crops: I. Variation in Net Assimilation Rate and Leaf Area between Species and Varieties, and within and between Years. *Annals of Botany*, 11(1), 41–76. <https://doi.org/10.1093/oxfordjournals.aob.a083148>